

## Strain distribution in a fold in the West Norwegian Caledonides

TIMOTHY B. HOLST

Department of Geology, University of Minnesota Duluth, Duluth, MN 55812, U.S.A.

and

HAAKON FOSSEN\*

Geologisk Institutt Avdeling A, Universitetet I Bergen, Allégaten 41, 5000 Bergen, Norway

(Received 13 October 1986; accepted in revised form 1 May 1987)

**Abstract**—Strain has been measured from clasts within a deformed conglomerate layer at 17 localities around an asymmetric fold in the Rundemanen Formation in the Bergen Arc System, West Norwegian Caledonides. Strain is very high and a marked gradient in strain ellipsoid shape exists. To either side of the fold, strain within the conglomerate bed is of the extreme flattening type. In the fold, especially on the lower fold closure, the strain is constrictional. Mathematical models of perturbations of flow in glacial ice have produced folds of the same geometry as this fold, with a strikingly similar pattern of finite strain. The fold geometry and strain pattern, as well as other field observations, suggest that the fold developed passively, as the result of a perturbation of flow in a shear zone, where the strain was accommodated by simple shear accompanied by extension along  $Y$ .

### INTRODUCTION

THE STATE of finite strain has proved to be a significant aid in the interpretation of folds and the folding process in rocks (e.g. Ramberg 1963, Fletcher 1974, Groshong 1975, Pfiffner 1980, Spang *et al.* 1980, Hudleston & Holst 1984). In recent years there has been considerable interest in folds developed in shear regimes and sheath folds (e.g. Carreras *et al.* 1977, Hudleston 1977, 1984, Quinquis *et al.* 1978, Minnigh 1979, Cobbold & Quinquis 1980, Ramsay 1980). Near Bergen, Norway, there is a Precambrian gneiss complex in which zones of intense shear developed during the Caledonian orogeny. A metasedimentary cover sequence to the gneiss is preserved in folds associated with these shear zones. A quartzite conglomerate bed within the metasedimentary sequence at one locality is preserved and exposed around an asymmetric mesoscopic fold. Using the conglomerate clasts as strain markers, the state of finite strain has been determined completely around the fold, and in the conglomerate to either side of the fold. The strain pattern contains interesting gradients in strain ellipsoid shape, and aids in the interpretation of the fold.

### GEOLOGIC SETTING

#### *The Bergen Arc System*

The Bergen Arc System (Kolderup & Kolderup 1940), a series of arcuate rock units surrounding Bergen, Norway, is bounded to the northeast by Precambrian basement (NW gneiss region), to the east by the Bergsdalen Nappes, and to the west by the North Sea (Fig. 1). Of the

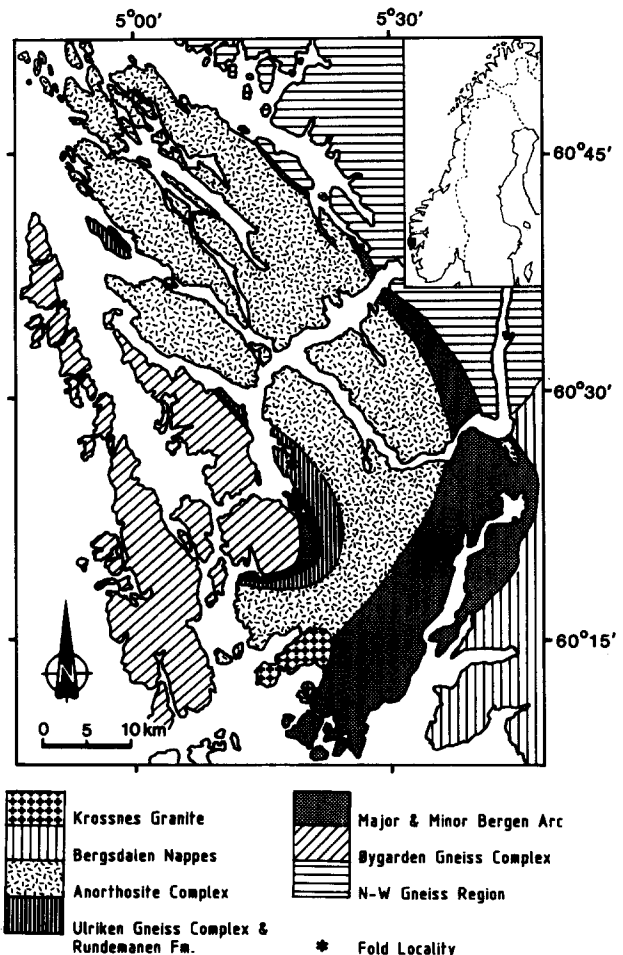


Fig. 1. Generalized geologic map of the Bergen Arc System (mainly after Kolderup & Kolderup 1940).

\* Present Address: Statoil, Postboks 1212, N-5001 Bergen, Norway.

rock units within the Bergen Arc System, the Øygarden Gneiss complex, the Anorthosite Complex and the Ulriken Gneiss Complex are all Precambrian rock complexes which have undergone Precambrian, as well as Caledonian deformation (Sturt & Thon 1978, Austrheim & Griffin 1985, Fossen 1986). The Krossnes Granite has been dated at  $453 \pm 50$  Ma (Brueckner 1972) and has been interpreted as synkinematic with the Scandian phase of Caledonian deformation (Fossen & Ingdahl 1987). The Major Bergen Arc is dominated by meta-igneous and metasedimentary rocks of lower Paleozoic age, including ophiolites (Furnes *et al.* 1980, Thon 1985). This rock complex has also suffered multiphase Caledonian deformation. The Minor Bergen Arc is a highly-deformed complex of meta-igneous rocks that exhibits characteristics of a dismembered ophiolite (Furnes *et al.* 1982), and also contains marine pelitic metasediments which may be part of a cap-rock to the ophiolite (Fossen 1986). In both Major and Minor Arcs, slices of basement gneisses and psammitic metasediments occur.

It is generally agreed that all of the components of the Bergen Arc System are allochthonous. However, there have been several different possible nappe stratigraphies suggested in the past few years (e.g. Sturt & Thon 1978, Bryhni & Sturt 1985, Gee *et al.* 1985, Ingdahl 1985, Fossen 1986). The Fanafjell Nappe of Sturt & Thon (1978) has been questioned by Fossen & Ingdahl (1987) who suggest an intrusive relationship for the Krossness Granite into the Gulefjellet Ophiolite. There is also no general agreement on the origin of the arcuate pattern of the rock complexes of the Bergen Arc System (e.g. Thon 1985, Fossen 1986).

### The Rundemanen Formation

The Rundemanen Formation (Fossen 1986) is a meta-sedimentary cover sequence, unconformably overlying the Ulriken Gneiss Complex. It is locally preserved in tight to isoclinal folds within shear zones in the Ulriken Gneiss Complex. The gneiss complex itself has undergone a complex history of Precambrian deformation and migmatization as well as Caledonian deformation.

Fossen (1986) outlines the following stratigraphy for the Rundemanen Formation. The lowest member, the Jordalen Member, contains an *in situ* weathering arkose up to a few metres thick at the basal unconformity. This passes upward to a quartzitic conglomerate with layers and lenses of coarse-grained arkose. Thickness of all members of the Rundemanen Formation are variable in the field, and true thickness is difficult to estimate because of the high and variable state of strain. The Jordalen Member is never more than about 8 m thick in exposure. The overlying Ramsli Member is a calcareous mica schist and semi-pelite which is in part diamictitic, with scattered pebble- to boulder-size clasts (lonestones) of gneissic, granitic, and quartzitic composition. It is up to 10 m thick in exposure. The uppermost member, the Rothaugen Member, is a sequence of quartzites and quartz-rich schists, up to 150 m thick in exposure.

No fossils have been found in the Rundemanen Formation, but based on lithological succession, Fossen (1986) offers a tentative correlation with the Eocambrian (Vendian) sparagmites of the Middle and Lower Allochthons in southeastern Norway.

Fossen (1986) recognized three periods of deformation which affected the Rundemanen Formation. The first episode was the most pronounced.  $F_1$  folds are tight to isoclinal, and an axial-planar  $S_1$  foliation has developed along with a stretching lineation. Intense shear accompanied the deformation, and small-scale  $F_1$  folds commonly show the removal of limbs by shear. The Rundemanen Formation is preserved in large-scale examples of these sheared  $F_1$  folds, each of which can be traced into intensely-sheared portions of the Ulriken Gneiss Complex, between which larger domains of less reworked gneiss are preserved. Open to tight  $F_2$  folds fold the  $S_1$  foliation and re-fold the  $F_1$  folds. An  $S_2$  crenulation cleavage and crenulation lineation are commonly developed.  $F_3$  structures are open, kink-like folds which re-fold  $F_2$  folds and which have been interpreted to be related to the formation of the arcuate structure of the Bergen Arc System (Fossen 1986).

### The Sandvikshytten Fold

One of the localities where the Rundemanen Formation has been preserved is near Sandvikshytten, about 3 km north of Bergen. Here a mesoscopic, SE-verging, asymmetric  $F_1$  fold is preserved. The fold is easily

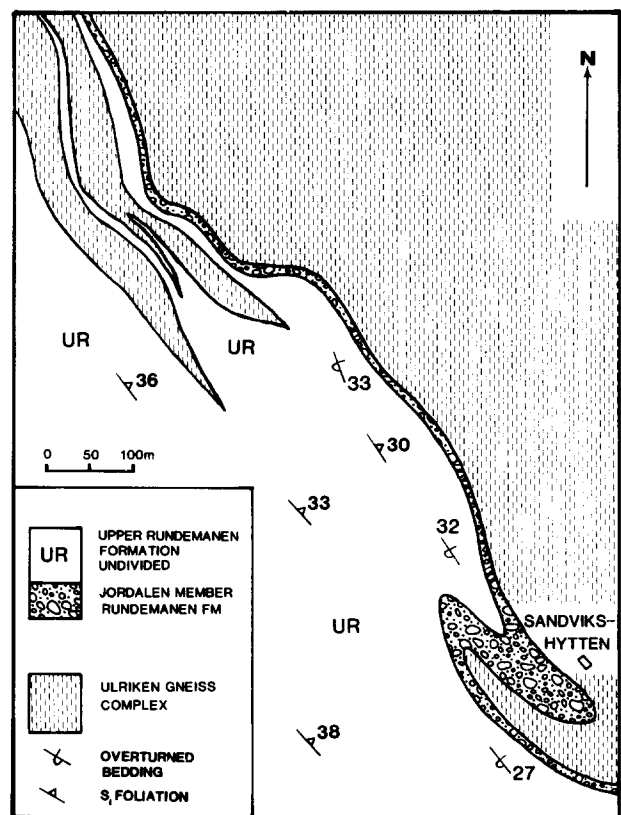


Fig. 2. Geologic map of the fold in the Jordalen Member of the Rundemanen Formation analyzed in this study. Map area bounded by UTM grid co-ordinates 270 025, 270 900; and 39 675, 40 350.

Strain distribution in a Norwegian fold

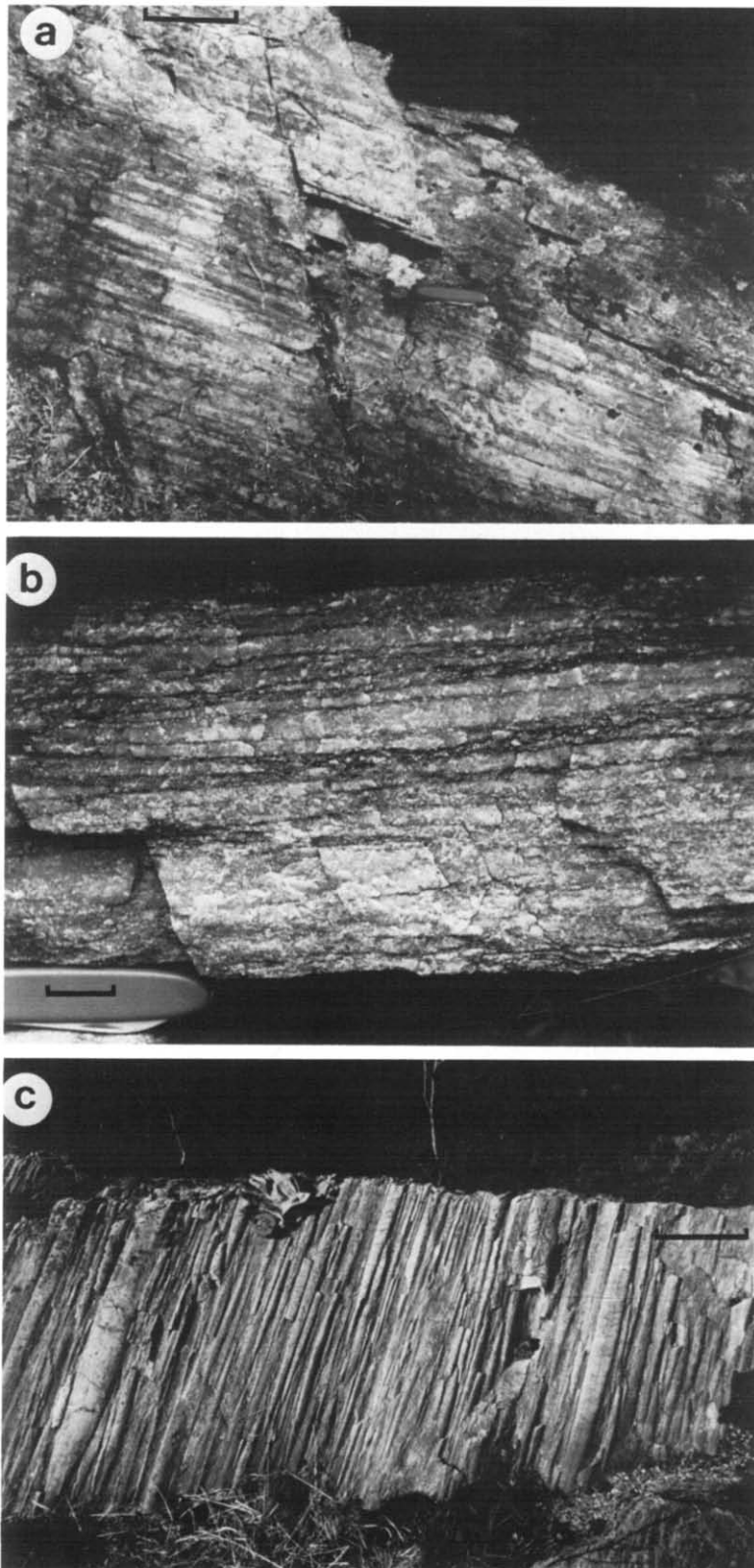


Fig. 3. Outcrop views showing markedly contrasting strain ellipsoid shapes. (a)  $Y-Z$  plane at locality 4, scale bar is 10 cm. (b)  $X-Z$  plane at locality 16, scale bar is 2 cm. (c)  $X-Y$  plane at locality 14, scale bar is 30 cm.



observed on a detailed geologic map, marked by the conglomeratic Jordalen Member of the Rundemanen Formation (Fig. 2). The asymmetric fold consists of two fold closures. The northeastern fold closure is herein referred to as the 'upper closure', and the southwestern closure as the 'lower closure'. To either side of the fold, bedding is overturned and dips gently to the ENE. The scale of the fold precludes measurement of axis or axial surface attitude in the field. Small-scale  $F_1$  folds are sheath folds, and indications of high shear strain present in the Rundemanen Formation and the underlying Ulriken Gneiss Complex suggest the Sandvikshytten fold is also sheath-like in three dimensions. The map view of the fold reveals a sub-similar fold geometry.

### STRAIN ANALYSIS

The clasts in the conglomerate in the Jordalen Member of the Rundemanen Formation consist entirely of quartzite and vein quartz. The matrix comprises less than 5% of the rock. The clasts were probably originally of the order of a few cm to tens of cm in dimension. Now they are highly strained, and commonly greater than 1 m in one or two dimensions (Fig. 3). There is some evidence of pressure solution, but most of the clasts do not have pressure-solved edges.

Gentle to steep slopes on the side of Sandviksfjellet provide adequate exposure of the conglomerate, and several joint sets provide sufficient broad planar two-dimensional exposures for clast examination. Three separate outcrop faces, each of different orientation and of sufficient extent to allow measurement of the requisite number of clasts, were generally available within a few metres of each other.

Measurements of shape and orientation of 100 clasts were recorded from each two-dimensional outcrop surface. Two-dimensional strain state was determined using standard  $R_f/\phi$  techniques (e.g. Ramsay 1967, Lisle 1985) and the polar plot (Elliott 1970, Holst 1982).

With two-dimensional strain data from three faces the three-dimensional strain may be determined (Ramsay 1967, Siddans 1980, Owens 1984). Three-dimensional strain was thus determined at 17 localities in the Jordalen conglomerate, at or near the Sandvikshytten fold (Fig. 4).

Some of the relevant three-dimensional strain parameters for the 17 strain localities are listed in Table 1. The strain ellipsoid shapes and orientations of the principal axes for the total data set are shown in Fig. 5. The data for each individual locality are shown on logarithmic deformation plots and Schmidt nets in Fig. 4.

### THE STRAIN PATTERN

Inspections of Table 1 and Figs. 4 and 5 reveal that strain is quite high at all localities. Ratios of  $X:Z$  vary from 13:1 to 36:1. The strain intensity parameters  $\bar{\epsilon}_s$  (Nadai 1963) and  $r$  (Watterson 1968) have been widely

Table 1. Calculated three-dimensional strain parameters for localities shown in Fig. 4

| Locality | $\epsilon_1 - \epsilon_2^*$ | $\epsilon_2 - \epsilon_3^*$ | $K^\dagger$ | $\nu^\ddagger$ | $\bar{\epsilon}_s^\S$ | $r^\parallel$ |
|----------|-----------------------------|-----------------------------|-------------|----------------|-----------------------|---------------|
| 1        | 0.03                        | 3.43                        | 0.01        | 0.98           | 2.82                  | 31.03         |
| 2        | 0.07                        | 3.30                        | 0.02        | 0.96           | 2.72                  | 27.07         |
| 3        | 0.04                        | 3.22                        | 0.01        | 0.98           | 2.64                  | 25.04         |
| 4        | 0.07                        | 3.33                        | 0.02        | 0.96           | 2.75                  | 28.07         |
| 5        | 0.14                        | 3.00                        | 0.05        | 0.90           | 2.51                  | 20.15         |
| 6        | 0.75                        | 2.20                        | 0.34        | 0.75           | 2.17                  | 10.11         |
| 7        | 0.96                        | 1.61                        | 0.60        | 0.25           | 1.83                  | 6.60          |
| 8        | 1.64                        | 1.25                        | 1.31        | -0.13          | 2.05                  | 7.64          |
| 9        | 0.56                        | 2.08                        | 0.27        | 0.79           | 1.97                  | 8.75          |
| 10       | 1.45                        | 1.39                        | 1.04        | -0.02          | 2.01                  | 7.25          |
| 11       | 1.95                        | 1.10                        | 1.77        | -0.28          | 2.18                  | 9.00          |
| 12       | 2.03                        | 0.92                        | 2.21        | -0.38          | 2.13                  | 9.10          |
| 13       | 2.69                        | 0.83                        | 3.24        | -0.53          | 2.60                  | 16.10         |
| 14       | 2.20                        | 1.38                        | 1.59        | -0.23          | 2.56                  | 12.00         |
| 15       | 1.76                        | 1.13                        | 1.56        | -0.22          | 2.06                  | 7.90          |
| 16       | 0.13                        | 2.64                        | 0.05        | 0.90           | 2.21                  | 14.14         |
| 17       | 0.05                        | 2.89                        | 0.02        | 0.96           | 2.38                  | 18.06         |

\*  $\epsilon_1 - \epsilon_2 = \ln X/Y$ ;  $\epsilon_2 - \epsilon_3 = \ln Y/Z$ ;  $X > Y > Z$ .

†  $K = (\epsilon_1 - \epsilon_2)/(\epsilon_2 - \epsilon_3)$  (Ramsay 1967, p. 329).

‡  $\nu = 1 - K/1 + K$  (Hossack 1968).

§  $\bar{\epsilon}_s = 1/\sqrt{3}[(\ln X/Y)^2 + (\ln Y/Z)^2 + (\ln Z/X)^2]^{1/2}$  (Nadai 1963).

||  $r = X/Y + Y/Z - 1$  (Watterson 1968).

used and both are given for comparison. The average value of  $\bar{\epsilon}_s$  for all 17 localities is 2.33, and for  $r$  the average value is 15.18. While the pattern of strain intensity and strain ellipsoid shape and orientation around the fold may be gleaned from Fig. 4, the pattern is made clear from the three groupings of localities given in Fig. 6.

Group I includes localities 1–5, 16 and 17. These are localities which are within the conglomerate bed on either side of the fold. Locality 5 is close to the upper limb of the upper fold closure, while locality 16 is close to the lower limb of the lower fold closure. Localities 1–4 and 17 are well removed from the fold. All seven of the localities in Group I have very high strains, and extremely oblate (flattened) strain ellipsoid shapes. Average values of the pertinent parameters for strain magnitude are  $\bar{\epsilon}_s = 2.58$ ,  $r = 23.37$ , and for strain ellipsoid shape,  $K = 0.03$ ,  $\nu = 0.95$ . Inspection of the Schmidt net for principal strain axis orientations for this group (Fig. 6a) shows that the least principal extension ( $Z$ ) has a consistent orientation for all seven of these locations, plunging about  $64^\circ/240^\circ$ . The  $X$  and  $Y$  axes are variably oriented in the plane perpendicular to  $Z$ . Outcrop views are shown in Fig. 3.

Group II consists of localities 6–10, which are on the upper fold closure (Fig. 4). In this group, strain magnitudes are lower (average  $\bar{\epsilon}_s = 2.01$ , average  $r = 8.07$ ) and strain ellipsoid shapes are variable. Three localities have strain ellipsoid shapes which fall within the flattening field (for no volume loss) and two ellipsoids fall into the constrictional field. The strain ellipsoids in the flattening field are not so extremely oblate as the seven localities of Group I. For Group II, average values for strain ellipsoid shape are  $K = 0.71$  and  $\nu = 0.32$ . Orientations of the principal axes of strain in this group are quite consistent;  $X$  plunges about  $22^\circ/098^\circ$ , and again  $Z$  plunges about  $64^\circ/240^\circ$ .

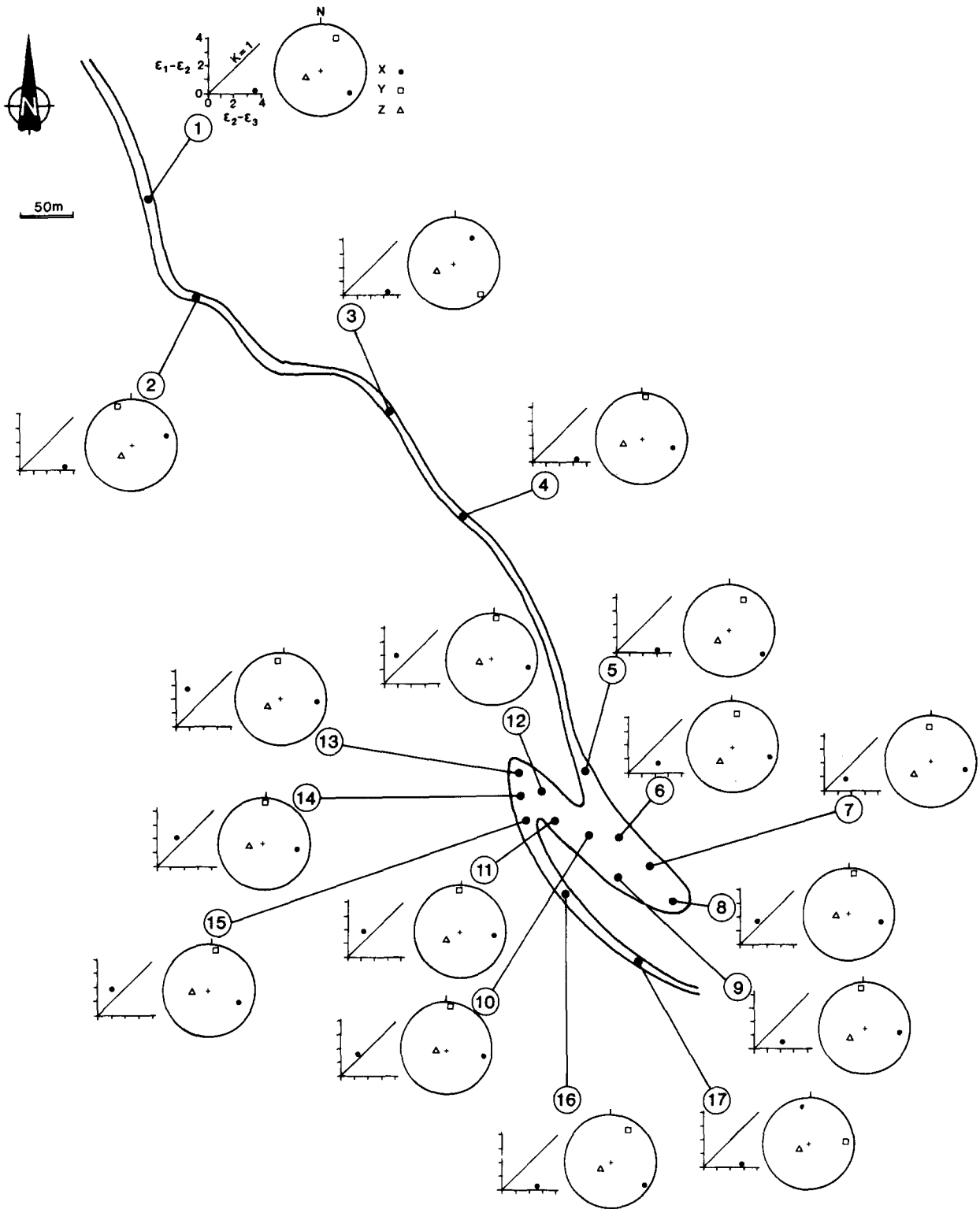


Fig. 4. Strain shape, amount and principal axes orientations displayed on logarithmic deformation plots and Schmidt nets for each of the 17 localities where finite strain was determined for this study. Keys to plots shown for locality 1.

Group III (localities 11–15, all on the lower fold closure) shows only constrictional (prolate) strain ellipsoids (Fig. 6c). The average value of  $K$  is 2.07, and average  $\nu = -0.32$ . Strain magnitudes are lower than Group I (average  $\bar{\epsilon}_s = 2.31$ , average  $r = 10.82$ ) but localities 13 and 14 have magnitudes as high as Group I. Orientations of the principal axes of strain are consistent, and essentially the same as that of Group II. Figure

3 shows an outcrop view of locality 14, which is representative of Group III.

### DISCUSSION AND CONCLUSIONS

Away from the fold there is an extremely high flattening strain. Within the fold, strains are generally some-

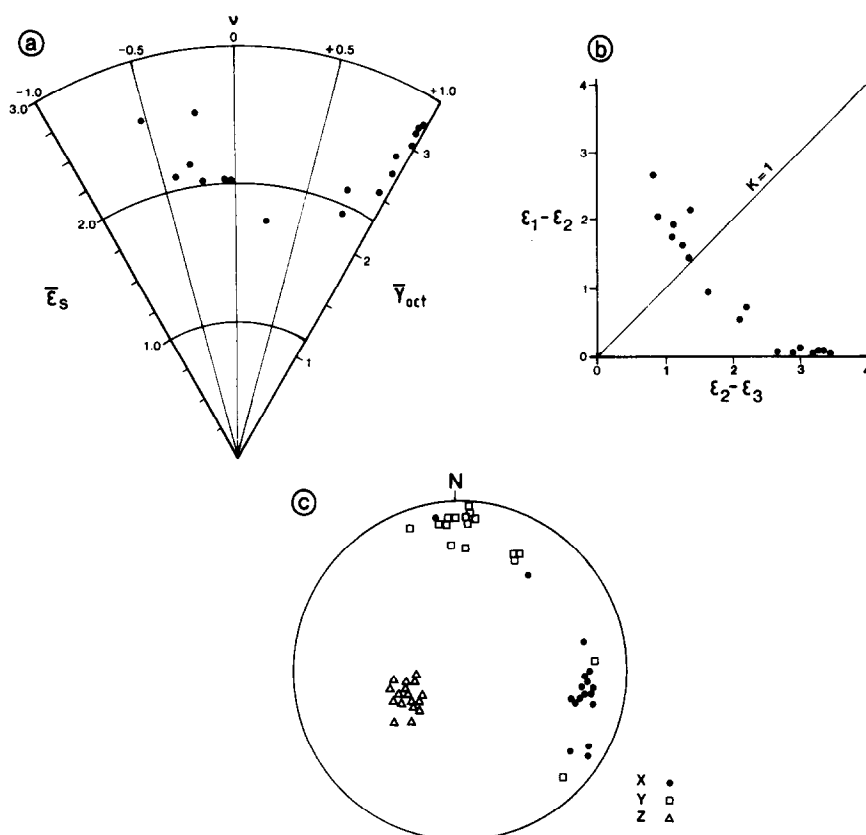


Fig. 5. Results of the strain determinations for all 17 localities. (a) Plot of the strain parameter  $\bar{\epsilon}_s$  vs Lode's parameter,  $\nu$  (see Hossack 1968). Also shown are values of  $\gamma_{\text{oct}}$ , the natural octahedral unit shear (Nadai 1963). (b) Logarithmic deformation plot (Ramsay 1967) of same data as (a). The line labelled  $K = 1$  is the locus of plane strain at constant volume. (c) Orientations of the principal axes of strain from the 17 locations shown on a Schmidt net.

what lower (although still high). On the upper fold closure strain ellipsoid shapes are variable, but clearly  $X$  is greater than  $Y$ . On the lower fold closure  $X$  is much greater than  $Y$ . This difference in strain ellipsoid shape is quite pronounced (Figs. 3 and 6) and exists over a small distance (a few metres to tens of metres). Such a high gradient in strain ellipsoid shapes at high strains is unusual.

The above observations are consistent with an interpretation that the fold formed passively from a perturbation of flow in a shear zone in which deformation was accommodated by simple shear accompanied by extension in the third dimension (the  $Y$  direction).

First, the Rundemanen Formation itself is preserved within shear zones in the Ulriken Gneiss Complex which are separated by zones of less sheared gneiss. A number of examples of small-scale  $F_1$  folds with limbs removed by shear exist in the Rundemanen Formation.

Hudleston (1976, 1977, 1983, 1984) has discussed the origin of folds in sheared ice (glaciers) and rocks, and has considered in some detail a mathematical model of the origin of folds in a glacier or ice cap. In steady-state flow in glaciers a banding and foliation forms, sub-parallel to the flow lines at high shear. This is analogous to a schistosity (and possibly transposition of bedding parallel to the schistosity) developing sub-parallel to the boundaries of a shear zone in rocks. If the steady-state

flow is perturbed, the banding or schistosity is no longer parallel to the flow lines. By introducing perturbations into steady-state flow in mathematical models of flow in glacial ice, Hudleston (1976, 1977) has produced passive folds of sub-similar geometry just down-glacier from the perturbation (Fig. 7). The geometry of this modelled fold is quite similar to that of the Sandvikshytten fold (Fig. 2).

Hudleston (1983) also considered in some detail the variations in finite strain caused by such a perturbation of steady-state flow in shear. Results vary depending on a number of influences including boundary conditions, but the result of particular interest here is the case of radial flow near the base of an ice cap. The steady-state strain in this case approximates that of simple shear with superimposed extension in the  $Y$  direction. Strain ellipsoid shapes are of the extreme oblate type with  $X \approx Y \gg Z$  (Fig. 8a). This is the type of strain in the Jordalen conglomerate away from the Sandvikshytten fold.

A perturbation of the steady-state flow may cause the  $XY$  plane of the cumulative (finite) strain to rotate through the shear plane (Fig. 8b). Subsequent flow causes the two-dimensional *finite* strain in the profile plane (perpendicular to the flow plane and parallel to the flow direction) to diminish, and a constrictional finite-strain ellipsoid develops with lower total strain magnitude (Fig. 8c). The  $X$  direction of the constrictional strain will lie within the shear plane and perpendicular to

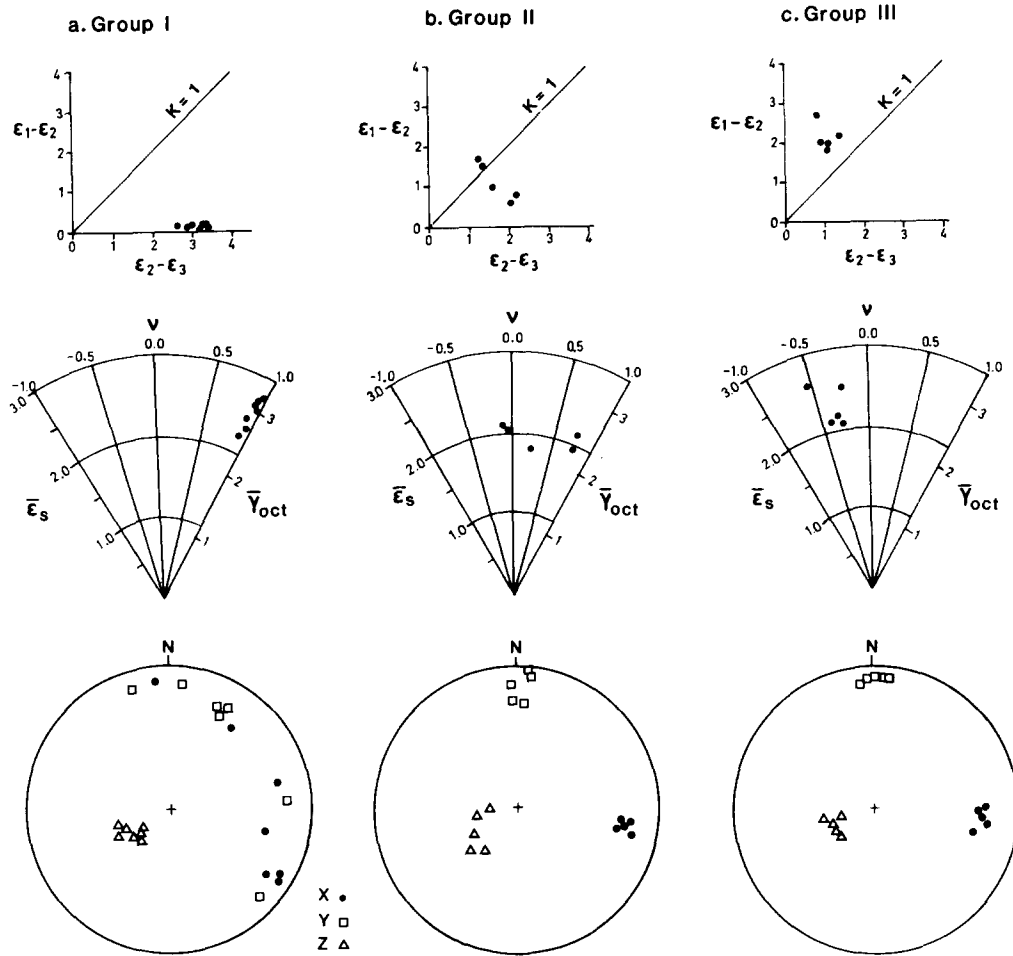


Fig. 6. Strain results plotted separately for Group I (localities 1-5, 16, 17); Group II (localities 6-10); and Group III (localities 11-15). Plots and parameters as for Fig. 5.

the flow direction. For a particular strain marker, continued flow will lead to higher strains in the profile plane, and less constrictional ellipsoids in three dimensions (Fig. 8d).

It is important to note that Hudleston (1983) pointed out that this zone of anomalous constrictional strain produced by such a perturbation is closely related to the passive fold in pre-existing layering or foliation which is also produced by the perturbation. He stated that the anomalous strain zone will 'lie in or adjacent to the hinges and overturned limb of such a fold' (Hudleston 1983, p. 462, and figs. 7 and 8). The strain pattern around the Sandvikshytten Fold fits the pattern predicted by Hudleston's modelling quite well.

The following history of development for the Sandvikshytten Fold is thus suggested. As fragments of the

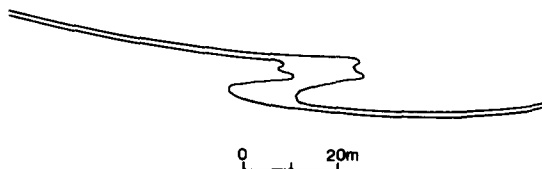


Fig. 7. Fold produced by numerical modelling of flow in an ice cap. From Hudleston (1977, fig. 3B) but of opposite vergence, for comparison with the Sandvikshytten fold.

Rundemanen Formation were incorporated into Caledonian shear zones within the Ulriken Gneiss Complex, high shear strain resulted in a schistosity parallel to the shear plane, and for the most part bedding also became transposed into this plane. The conglomeratic bed could easily have undergone tectonic thinning.

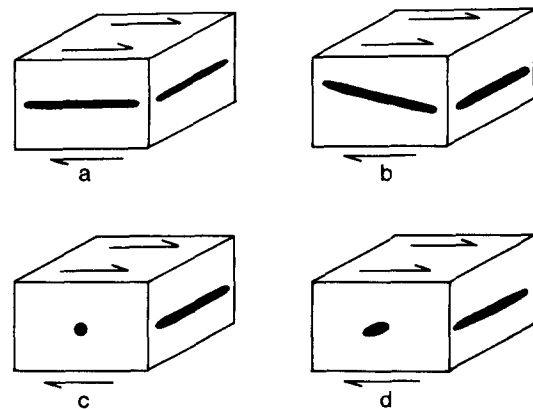


Fig. 8. The development of constrictional strains after a perturbation of flow in a shear zone. Strains are diagrammatic. (a) Strain prior to perturbation, simple shear with extension in the third dimension. (b) Rotation of strain marker below shear plane due to flow perturbation. (c) Progressive shear results in constrictional strain. (d) As shear continues strain becomes less strongly constrictional.



Strain in general was accommodated by simple shear accompanied by extension parallel to  $Y$  so that an oblate strain ellipsoid developed. At the Sandvikshytten locality, the orientation of bedding on either side of the fold (Fig. 2) and the geometry of the principal axes of strain (Figs. 5 and 6) suggest that the shear zone here strikes approximately  $150^\circ$  and dips  $25\text{--}35^\circ$  to the NE.

Because of a perturbation of the flow in the shear zone on the SW side of the zone, the bedding was deflected from parallelism with the flow lines in the shear zone, and a passive fold (the Sandvikshytten Fold) developed, verging 'downstream' from the perturbation. The vergence of the fold indicates dextral shear within the shear zone in map view. This is consistent with microscopic kinematic indicators such as asymmetric augen structures around feldspar porphyroclasts (Simpson & Schmid 1983) from the Ulriken Gneiss Complex near the contact with the Jordalen conglomerate. It is tempting to suggest that the slices of Ulriken Gneiss within the Rundemanen Formation (on the correct side of the shear zone and in the correct position just 'upstream' from the fold) are the cause of the perturbation, but there are various ways of introducing perturbations into the flow in shear zones in rocks (Cobbold & Quinquis 1980, Hudleston 1983, 1984), and some other less obvious perturbation may exist here.

Because of the perturbation, finite-strain markers within the fold rotated through the shear plane, and continued flow in the shear zone led to the phenomenon observed in Fig. 8. Constrictional strains are most pronounced in the lower fold closure (Figs. 4 and 6) but clearly strains in the upper closure are also anomalous compared to the strains on either side of the fold (Fig. 6a & b). The  $X$  direction of the constrictional strain in the fold consistently plunges about  $22^\circ/098^\circ$ . As measured by the strain magnitude parameters  $\bar{\epsilon}_s$  and  $r$ , the strains in the fold are also lower (for the most part) than strains to either side (Table 1), as predicted by Hudleston's model.

The mechanism suggested here is not that of rolling of competent pebbles so that their long axes lie normal to the transport direction. While it is true that in the mechanism suggested in this paper the zone of anomalous strain will contain constrictional strain and pebbles will lie with long axes normal to the shear direction, the mechanism is entirely different from the idea of rolling of pebbles. In the mechanism described in this paper, the pebbles are passive strain markers of the ductile deformation, and the zone of anomalous constrictional strain is caused solely by the perturbation of the flow in the shear zone.

Other areas of contrasting strain ellipsoid shape exist in the Caledonides (e.g. Hossack 1968). We do not suggest that they have been formed by the same mechanism we are postulating for the Sandvikshytten locality. The geometry and vergence of the Sandvikshytten fold, together with other indications of high shear, suggest that the fold developed passively in shear. Such an interpretation is strongly supported by the unusual pattern of finite strain around the fold, which would be

problematic without this explanation. Such strain patterns may well be common in passive folds developed in shear zones in rocks as suggested by Hudleston (1983), but examples such as the Sandvikshytten fold, where strain markers exist around a fold to document the pattern, seem to be rare.

*Acknowledgements*—This research was supported in part by a Fulbright Senior Research Fellowship (T. B. Holst) and a Bush Sabbatical Fellowship from the University of Minnesota (T. B. Holst).

## REFERENCES

- Austrheim, H. & Griffin, W. L. 1985. Shear deformation and eclogite formation within granulite-facies anorthosites of the Bergen Arcs, western Norway. *Chem. Geol.* **50**, 267–281.
- Brueckner, H. K. 1972. Interpretation of Rb/Sr ages from the Precambrian and Proterozoic rocks of southern Norway. *Am. J. Sci.* **272**, 334–358.
- Bryhni, I. & Sturt, B. A. 1985. Caledonides of southwestern Norway. In: *The Caledonide Orogen and Related Areas* (edited by Gee, G. D. & Sturt, B. A.). Wiley, New York, 89–107.
- Carreras, J., Estrada, A. & White, S. 1977. The effects of folding on the  $c$ -axis fabrics of a quartz mylonite. *Tectonophysics* **39**, 3–24.
- Cobbold, P. R. & Quinquis, H. 1980. Development of sheath folds in shear regimes. *J. Struct. Geol.* **2**, 119–126.
- Elliott, D. 1970. Determination of finite strain and initial shape from deformed elliptical objects. *Bull. geol. Soc. Am.* **81**, 2221–2236.
- Fletcher, R. C. 1974. Wavelength selection in the folding of a single layer with power-law rheology. *Am. J. Sci.* **274**, 1029–1043.
- Fossen, H. 1986. Structural and metamorphic development of the Bergen area, west Norway. Unpublished Cand. Scient. thesis, University of Bergen.
- Fossen, H. & Ingdahl, S. E. 1987. An investigation of the Krossnes granite (Fanafjell nappe) and a reevaluation of its tectonostratigraphic position in the Bergen Arc System, west Norway. *Norsk geol. Tidsskr.* **67**, 59–66.
- Furnes, H., Roberts, D., Sturt, B. A., Thon, A. & Gale, G. H. 1980. Ophiolite fragments in the Scandinavian Caledonides. *Proc. Int. Ophiolite Symp.*, Cyprus, 582–600.
- Furnes, H., Thon, A., Nordås, J. & Garmann, L. B. 1982. Geochemistry of Caledonian metabasalts from some Norwegian ophiolite fragments. *Contr. Miner. Petrol.* **79**, 295–307.
- Gee, D. G., Kumpulainen, R., Roberts, D., Stephens, M. B., Thon, A. & Zachrisson, E. 1985. Scandinavian Caledonides, tectonostratigraphic map. In: *The Caledonide Orogen and Related Areas* (edited by Gee, D. G. & Sturt, B. A.). Wiley, New York.
- Groshong, R. H., Jr. 1975. Strain, fractures and pressure solution in natural single-layer folds. *Bull. geol. Soc. Am.* **86**, 1363–1376.
- Holst, T. B. 1982. The role of initial fabric on strain determination from deformed ellipsoidal objects. *Tectonophysics* **82**, 329–350.
- Hossack, J. R. 1968. Pebble deformation and thrusting in the Bygdin area (southern Norway). *Tectonophysics* **5**, 315–339.
- Hudleston, P. J. 1976. Recumbent folding in the base of the Barnes Ice Cap, Baffin Island, Northwest Territories, Canada. *Bull. geol. Soc. Am.* **87**, 1684–1692.
- Hudleston, P. J. 1977. Similar folds, recumbent folds and gravity tectonics in ice and rocks. *J. Geol.* **85**, 113–122.
- Hudleston, P. J. 1983. Strain patterns in an ice cap and implications for strain variations in shear zones. *J. Struct. Geol.* **5**, 455–463.
- Hudleston, P. J. 1984. Generation of folds in shear zones. *Geol. Soc. Am. (Abst. with Programs)* **16**, 546.
- Hudleston, P. J. & Holst, T. B. 1984. Strain analysis and fold shape in a limestone layer and implications for layer rheology. *Tectonophysics* **106**, 321–347.
- Ingdahl, S. E. 1985. Stratigraphy, structural geology, and metamorphism in the Os area, Major Bergen Arc. Unpublished Cand. Scient. thesis, University of Bergen.
- Kolderup, C. F. & Kolderup, N. H. 1940. Geology of the Bergen Arc System. *Bergens Mus. Skr.* **20**, 1–137.
- Lisle, R. J. 1985. *Geological Strain Analysis*. Pergamon Press, Oxford.
- Minnigh, L. D. 1979. Structural analysis of sheath folds in a metachert from the Western Italian Alps. *J. Struct. Geol.* **1**, 275–282.
- Nadai, A. 1963. *Theory of Flow and Fracture of Solids*. Engineering Societies Monographs. McGraw-Hill, New York.
- Owens, W. H. 1984. The calculation of a best-fit ellipsoid from

- elliptical sections on arbitrarily oriented planes. *J. Struct. Geol.* **6**, 571–578.
- Pfiffner, O. A. 1980. Strain analysis in folds (Infrahelvetic complex, Central Alps). *Tectonophysics* **61**, 337–362.
- Quinquis, H., Audren, C. L., Brun, J. P. & Cobbold, P. R. 1978. Intense progressive shear in the Ile de Groix blueschists. *Nature, Lond.* **273**, 43–45.
- Ramberg, H. 1963. Strain distribution and geometry of folds. *Bull. geol. Instn. Univ. Uppsala* **42**, 1–20.
- Ramsay, J. G. 1967. *Folding and Fracturing of Rocks*. McGraw-Hill, New York.
- Ramsay, J. G. 1980. Shear zone geometry: a review. *J. Struct. Geol.* **2**, 83–99.
- Siddans, A. W. B. 1980. Analysis of three-dimensional homogeneous finite strain using ellipsoidal objects. *Tectonophysics* **64**, 1–16.
- Simpson, C. & Schmid, S. M. 1983. An evaluation of criteria to deduce the sense of movement in sheared rocks. *Bull. geol. Soc. Am.* **94**, 1281–1288.
- Spang, J. H., Simony, P. S. & Mitchell, W. J. 1980. Strain and folding mechanisms in a similar style fold from the northern Selkirks of the Canadian Cordillera. *Tectonophysics* **66**, 253–267.
- Sturt, B. A. & Thon, A. 1978. Caledonides of Southern Norway. In: *Caledonian–Appalachian Orogen of the North Atlantic Region*. IGCP Project 27. *Geol. Surv. Pap. Can.* **78-13**, 39–47.
- Thon, A. 1985. The Gulefjellet Ophiolite Complex and the structural evolution of the Bergen Arcs, West Norwegian Caledonides. In: *The Caledonide Orogen and Related Areas* (edited by Gee, D. G. & Sturt, B. A.). Wiley, New York, 671–677.
- Watterson, J. 1968. Homogeneous deformation of the gneisses of Vesterland, southwest Greenland. *Meddr Grønland* **175**, 1–75.